

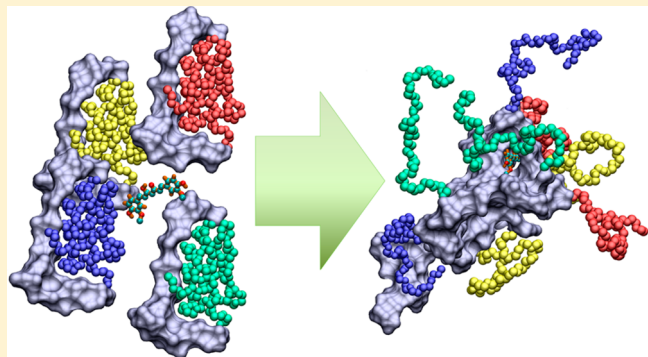
Interaction of Curcumin with PEO–PPO–PEO Block Copolymers: A Molecular Dynamics Study

Susruta Samanta and Danilo Roccatano*

School of Engineering and Science, Jacobs University Bremen, Campus Ring 1, 28759, Bremen, Germany

Supporting Information

ABSTRACT: Curcumin, a naturally occurring drug molecule, has been extensively investigated for its various potential usages in medicine. Its water insolubility and high metabolism rate require the use of drug delivery systems to make it effective in the human body. Among various types of nanocarriers, block copolymer based ones are the most effective. These polymers are broadly used as drug-delivery systems, but the nature of this process is poorly understood. In this paper, we propose a molecular dynamics simulation study of the interaction of Curcumin with block copolymer based on polyethylene oxide (PEO) and polypropylene oxide (PPO). The study has been conducted considering the smallest PEO and PPO oligomers and multiple chains of the block copolymer Pluronic P85. Our study shows that the more hydrophobic 1,2-dimethoxypropane (DMP) molecules and PPO block preferentially coat the Curcumin molecule. In the case of the Pluronic P85, simulation shows formation of a drug–polymer aggregate within 50 ns. This process leaves exposed the PEO part of the polymers, resulting in better solvation and stability of the drug in water.



INTRODUCTION

Curcumin, a polyphenol derived from the root of turmeric (*Curcuma longa*) is widely used as a dietary spice and natural food coloring agent throughout the world.^{1,2} It also finds its place in the traditional Indian medicine system, Ayurveda, for its wide ranged therapeutic applications as an antibiotic, anti-inflammatory, antirheumatic, antiarthritic, and antioxidant agent and as a cure for several other diseases.^{3,4} Recent studies reveal that Curcumin has potent anticancer effects both alone or with other anticancer drugs.^{5,6} This has been tested *in vivo* and *in vitro* with melanoma, mantle cell lymphoma, hepatic, prostatic, ovarian, and pancreatic carcinomas.⁷ Curcumin has been reported to have diverse effects on signaling molecules down-regulation of the expression of angiogenesis-associated genes, activation of the apoptotic mechanisms, and induction of the cell cycle arrest.⁸ It also enhances chemotherapeutic responses of cancer cells to several anticancer drugs.^{5,9} Curcumin is a potential inhibitor of the nuclear factor kappaB (NF- κ B) signaling pathway.¹⁰ NF- κ B promotes carcinogens in liver, colon, lung, and leukemia and prostate cancer, and NF- κ B excess is a main reason for the failure of chemotherapy with many drugs as well.¹¹ Curcumin also prevents accumulation of amyloid- β (A β) aggregates as soluble oligomers, hence preventing Alzheimer's disease.^{12–14}

In spite of the aforementioned therapeutic potentials, low solubility in water and high degradation rate hinder the clinical development of Curcumin. It is not soluble in water at neutral or acidic pH and dissociates in alkaline conditions.^{15,16} A

clinical study on rats revealed the disappearance of Curcumin from blood in 1 h after a dose of 40 mg/kg scale and confirms only 10 ng/mL serum concentration upon 2 g of oral dose.^{17,18} For these reasons, there is a need to associate the drug with a delivering carrier to prevent these problems.

Amphiphilic block copolymers which can assemble to form a micelle can be used as a carrier of poorly soluble drug molecules to cells.^{19–21} Different studies of Curcumin with different amphiphilic block copolymer based carriers have been reported in the literature.^{22–27} They increase solubility, improve stability, and control the release profile. In particular, polyethylene oxide (PEO) and polypropylene oxide (PPO) based triblock copolymers, Pluronics, are among the most effective carriers for Curcumin.²⁷ In particular, PEO_n–PPO_m–PEO_n type Pluronics (also known as Poloxamers) are widely used in drug delivery. When in water, the PPO parts form a core with flanking PEO parts which helps stabilize the polymer in water and increases solubility.

Pluronics are nontoxic, inexpensive, and easily customizable polymers.²¹ Moreover, they have tendencies to accumulate in tumor cells, enhance the efficiency of chemotherapeutics, and decrease the chances of side effects on the immune system.^{28,29}

However, the molecular mechanics of the interaction of the polymers with drugs and their delivery at the molecular level

Received: September 24, 2012

Revised: February 22, 2013

are not yet clearly understood. So far, experimental studies on these topics for Curcumin are very limited, and there are no theoretical investigations present in the literature.

In this work, using molecular dynamics simulations, we aim to understand the interaction of Curcumin with polymer surfactants based on PEO/PPO units. In particular, we have studied the interaction of the drug molecule with the Pluronic P85 (PEO₂₅–PPO₄₀–PEO₂₅). P85 is a variant of Pluronic with high hydrophilic–lipophilic balance and has a molar ratio of 1.03 for PEO/PPO units. The “hydrophilic lipophilic balance” (HLB) ratio for P85 is 17. This value is comparable to the Pluronic F68 (HLB ratio = 17.8) and F127 (HLB ratio = 24) which were used by Sahu et al. to experimentally study the encapsulation of Curcumin in Pluronics.²⁷ Furthermore, this model has previously been extensively tested in different solvent conditions and performed satisfactorily.³⁰

In addition, interactions of the drug molecule with 1,2-dimethoxyethane (DME) and 1,2-dimethoxyp propane (DMP), which are the smallest oligomers of PEO and PPO, have been studied. The Curcumin model has been tested with simulations in water, methanol, and 1-octanol.

In this article, the details of the force fields and methodologies used are described in the Methods section. The results of the simulations of Curcumin in water, methanol, 1-octanol, and DME/DMP/water mixture and in the presence of Pluronic P85 are explained in the Results and Discussions section. Finally, in the Conclusions section, the findings of this work have been summarized.

METHODS

Force Field. Figure 1 shows the chemical structure of Curcumin ((1E,6E)-1,7-bis(4-hydroxy-3-methoxyphenyl)-1,6-

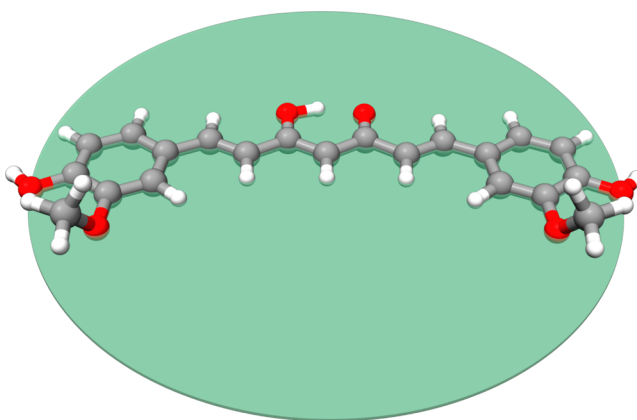


Figure 1. Optimized structure of Curcumin. The carbon atoms are shown in dark gray, oxygen atoms in red, and hydrogen atoms in white. The green plane helps to understand the planarity of the molecules.

heptadiene-3,5-dione). It exhibits keto–enol tautomerization, and depending upon the solvent, the enol form can constitute up to 95% of the conformations.³¹ Quantum mechanical calculations were performed on the enol form of the molecule to obtain the optimized structure and the partial charges of the atoms. Geometry optimization was done using the restricted B3LYP method with the 6-31G** basis set, and the atomic charges were calculated using the ChelpG procedure.³² The optimized structure of Curcumin is shown in Figure 1. The coordinates of the atoms of the optimized structure and their

corresponding partial charges are reported in Tables S1 and S2 of the Supporting Information (SI). For the Curcumin model, parameters for partial charges, bond lengths, bond angles, and dihedral angles were based upon the QM calculations (Tables S3–S5 in the SI). The force constants for the bond angles and the torsional interactions and the Lennard-Jones parameters were adapted from the GROMOS96 parameters. The quality of the model was tested by calculating its partition coefficient in the water/1-octanol system ($\log P_{\text{octanol/water}}$) following the method explained in our previous publication.³³ For the DME, DMP, and P85 polymer, the recent models by Hezaveh et al.^{30,34} were used. The simple point charge (SPC)³⁵ model for water and the OPLS united atom (OPLS-UA) model for methanol³⁶ and 1-octanol³⁷ were used.

Simulation Setup. The quantum mechanical calculations were performed using the Gaussian 03 program.³⁸ All the molecular dynamics simulations were performed using GROMACS (version 4.5.5)³⁹ software package, and VMD⁴⁰ was used for visualization purposes. Details of the simulated systems are shown in Table 1. For all the simulations, the

Table 1. Description of the Systems Simulated^a

system	components (number of molecules in parentheses)	box size ($x \times y \times z$)/nm ³	number of atoms
A	(1) Curcumin + (4124) water	5 × 5 × 5	12408
B	(1) Curcumin + (1866) methanol	5 × 5 × 5	5634
C	(1) Curcumin + (413) 1-octanol	5 × 5 × 5	4166
D	(1) Curcumin + (23) DME + (24) DMP + (2695) water	4.5 × 4.5 × 4.5	8427
E	(1) Curcumin + (1) P85 + (6917) water	6 × 6 × 6	21106
F	(1) Curcumin + (8) P85 + (22393) water	9 × 9 × 9	69767
G	(8) P85 + (22393) water	9 × 9 × 9	69731

^aSystems A–E were simulated for 50 ns; systems F and G were simulated for 100 ns.

temperature was kept constant at 298 K using the V-rescale thermostat⁴¹ with a coupling constant of 0.1 ps. The pressure was maintained constant at 1 bar using a Berendsen barostat⁴² with a coupling constant of 0.5 ps. The bond lengths were constrained using the LINCS⁴³ algorithm. An integration time step of 2 fs was used for all the simulations. Electrostatic interactions were evaluated using the particle mesh Ewald method⁴⁴ with a real space cutoff of 1.0 nm, grid spacing of 0.12 nm, and a fourth-order spline interpolation. Lennard-Jones interactions were truncated at 1.0 nm.

Calculation of the Spatial Density Distribution. The spatial density distribution of the solvent molecules around the Curcumin molecule was calculated using the *g_spatial* program of the GROMACS package. A cubic grid with 0.1 nm grid spacing was used for all the calculations. The solvent molecules were centered around the Curcumin molecule in each trajectory frame using a translational–rotational fit to the first configuration of the MD trajectory and removing the periodic boundary conditions. Finally, the atomic positions of the selected atoms of solvent molecules were mapped on a cubic grid centered on the geometric center of the Curcumin molecule and averaged with respect to the number of frames analyzed. The averaged volumetric density data obtained were analyzed using the program VMD.

Calculation of Free Energy of Solvation (ΔG) and Partition Coefficient ($\log P_{\text{octanol/water}}$). The final frames of

the simulation of Curcumin in water, methanol, and 1-octanol (for 50 ns) were taken as the starting structures for the calculation of free energy of solvation. Gibbs free energy of solvation in water (ΔG_{hyd}), in methanol (ΔG_{met}), and in 1-octanol (ΔG_{oct}) at 298 K was calculated using the thermodynamic integration (TI) method.⁴⁵ The TI integration was performed on 21 λ points: 0, 0.05, 0.1, 0.15, 0.2, 0.25, 0.3, 0.35, 0.4, 0.45, 0.5, 0.55, 0.6, 0.65, 0.7, 0.75, 0.8, 0.85, 0.9, 0.95, and 1.00. The soft-core parameters α and σ were assigned the values of 1.5 and 0.30, respectively. For each λ -point, the equilibrated system was run for 2 ns. From ΔG_{hyd} and ΔG_{oct} at the temperature T , the corresponding partition coefficient is calculated according to the following formula³⁷

$$\log P_{\text{octanol/water}} = \frac{\Delta G_{\text{hyd}} - \Delta G_{\text{oct}}}{2.303RT} \quad (1)$$

where R is the universal gas constant.

RESULTS AND DISCUSSION

Simulation of Curcumin in Water, Methanol, and 1-Octanol. The values of free energies resulted in $\Delta G_{\text{hyd}} = 4.6 \pm 1.1$ kJ/mol, $\Delta G_{\text{met}} = -5.3 \pm 0.9$ kJ/mol, and $\Delta G_{\text{oct}} = -2.1 \pm 0.6$ kJ/mol. The free energy of solvation value indicates insolubility of Curcumin in water and better solubility in methanol than in 1-octanol. This is in agreement with the available chemical information.

The value of $\log P_{\text{octanol/water}}$ resulted in 1.17. Unfortunately, there are no experimental chemical data that can be used to verify the results of our MD simulations. However, theoretically calculated values of $\log P_{\text{octanol/water}}$ result in 3.07 ± 0.4 ⁴⁶ or 2.517 (using the CONFLEX/PM3 method).⁴⁷ Qualitatively, the values are in agreement and indicate Curcumin's higher affinity toward 1-octanol than water.

To understand the behavior of Curcumin in simple solutions, it was simulated in water, in methanol, and in 1-octanol. Figure 2 shows the spatial distribution of solvent atoms around the Curcumin molecule during a 50 ns free simulation. As expected, the solvent molecules tend to gather around the hydrophilic

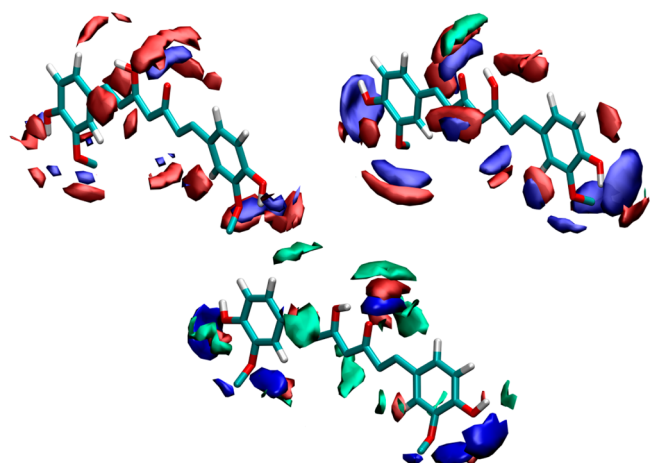


Figure 2. Spatial distribution of solvent atoms around the Curcumin molecule in water (top left), methanol (top right), and 1-octanol (bottom). Hydrogen atoms are shown in blue, oxygen atoms in red, and carbon atoms in green. Contour values of the iso-surfaces are 20 for both hydrogen and oxygen of water and 35 for all three types of atoms in methanol. Isovalue for 1-octanol carbon is 20, and those for 1-octanol oxygen and hydrogen are 200.

and polar region of Curcumin. High density of solvent hydrogen atoms around the oxygen atoms of Curcumin indicates a good extent of hydrogen bonding with the solvent molecules.

Figure 3 shows the root-mean-square fluctuation (RMSF) per atom plot of the Curcumin molecule during a 50 ns free

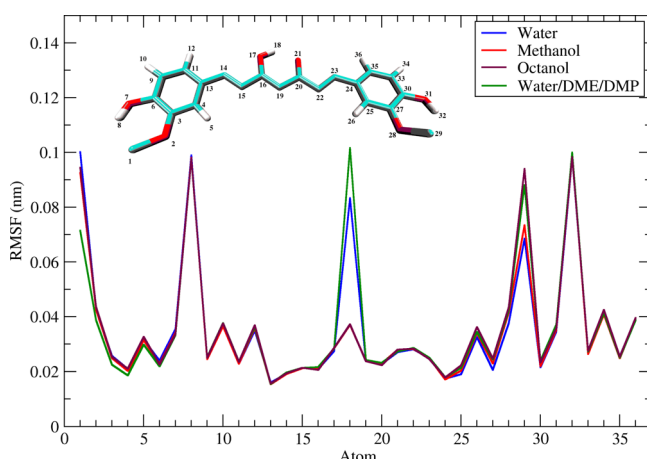


Figure 3. Root-mean-square fluctuation (RMSF) of the atoms of Curcumin in water (blue), methanol (red), and 1-octanol (maroon) and in the presence of DME and DMP in water (green). The atom numbers are shown in the inset.

simulation in different solvent conditions—in water, in methanol, in 1-octanol, and in water with DME and DMP. As expected, five major fluctuations are seen in the molecule, and they correspond to the three $-\text{OH}$ groups and two $-\text{OCH}_3$ groups. In the case of methanol and 1-octanol, only four major fluctuations are seen—all in the $-\text{OH}$ and $-\text{OCH}_3$ groups attached to the phenyl rings. The enol hydroxyl group remains stable resulting in low RMSF per residue. This implies that the rotation along the O-H bond is restricted in methanol and 1-octanol.

To further evaluate the scenario, the average distance between the enol hydrogen and keto oxygen was calculated. Figure 4 shows the distribution of average distance of the enol hydrogen and the keto oxygen of Curcumin during a 50 ns free

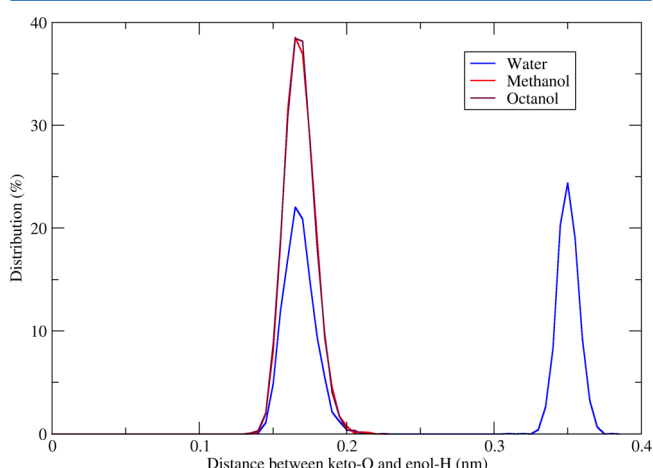


Figure 4. Distribution of average distance between the enol hydrogen (atom number 18) and the keto oxygen (atom number 21) in water, methanol, and 1-octanol.

simulation in water, methanol, and 1-octanol. In methanol and 1-octanol, we observe a single peak at 0.16 nm, but in water, we observe a bimodal distribution having a peak at the same position as of methanol and a second peak at 0.35 nm. In methanol and 1-octanol, the enol hydrogen tends to point toward the keto oxygen (as seen in Figure 2), but in water, though mostly its conformation is the same, there is a significant contribution of the conformer where the hydrogen points away from the keto oxygen atom (as seen in Figure 2).

Figure 5 shows the hydrogen bonding between Curcumin and solvent molecules. From the figure, we can observe that the

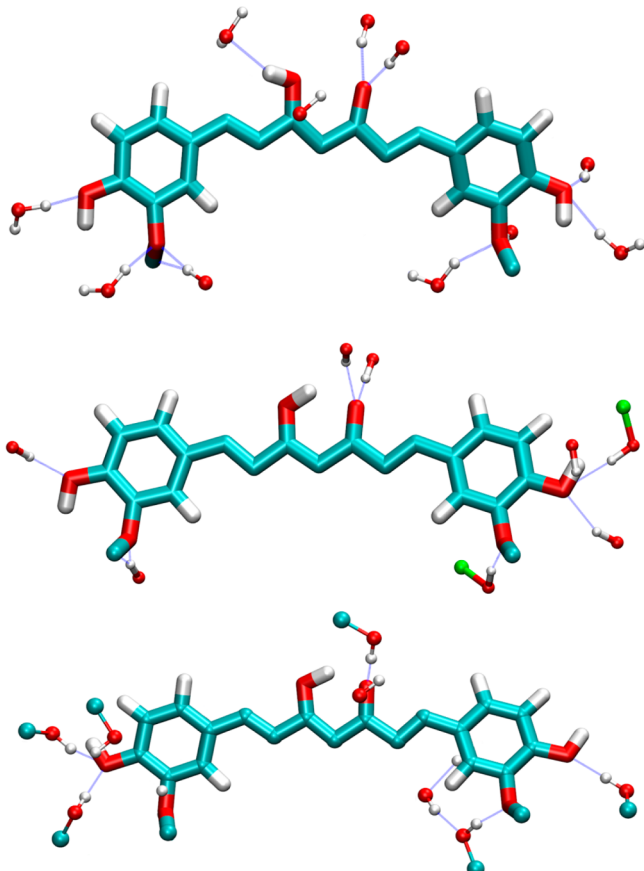


Figure 5. Hydrogen bonding of Curcumin in water (top), in methanol (middle), and in 1-octanol (bottom).

oxygen of water tends to form a hydrogen bond with the enolic hydrogen of Curcumin. As a result, the O–C bond is rotated, and the hydrogen atom faces away from the keto oxygen atom. Methanol and 1-octanol oxygen being less electronegative cannot form this type of hydrogen bond, and hence, the enolic hydrogen always keeps facing the keto oxygen of the Curcumin molecule.

The radial distribution function (RDF) of the oxygen atoms of the solvent molecules with respect to the two types of rings present in the Curcumin molecule is shown in Figure 6. RDF was calculated with respect to the ring formed by six central atoms (as shown in Figure 6) and one of the phenyl rings. The positions of the first peaks in all the cases have a lower value for methanol and 1-octanol than that of water, indicating the hydrophobic nature of the molecule. The high value of RDF for 1-octanol indicates a high attractive interaction between 1-octanol and Curcumin. From the RDF curves, it is clear that

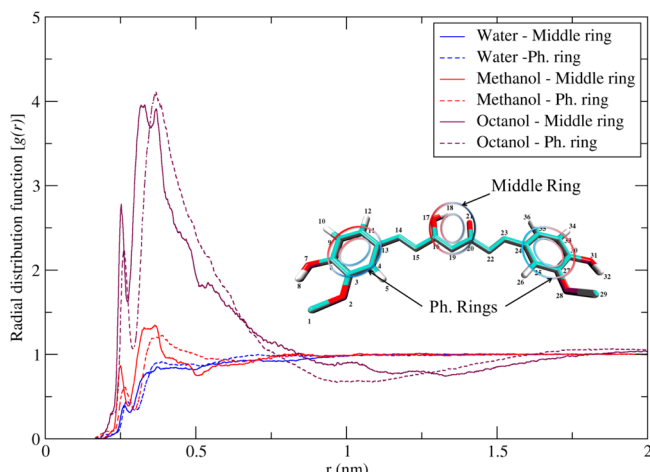


Figure 6. Radial distribution function of the oxygen atoms of the solvent molecules with respect to the two different types of rings in the Curcumin molecule.

water has the least attractive interaction with Curcumin between the three solvents used for simulation. For all the solvents, the first peak for the nonpolar phenyl rings is shifted to longer distance than that of the polar middle ring, indicating more interaction with the middle ring. The same was observed from the spatial distribution of solvent atoms around the drug molecule (Figure 2). The average number of contacts (N_{cont}) between the Curcumin molecule and the solvent molecules was found to be 82 (± 3) for water, 40 (± 2) for methanol, and 26 (± 3) for 1-octanol.

The diffusion coefficient value in water, methanol, and 1-octanol was found to be $2.61 (\pm 0.24) \times 10^{-9} \text{ m}^2/\text{s}$, $1.17 (\pm 0.07) \times 10^{-9} \text{ m}^2/\text{s}$, and $0.53 (\pm 0.01) \times 10^{-9} \text{ m}^2/\text{s}$, respectively. The restricted mobility of the Curcumin molecule indicates stronger interactions with methanol and 1-octanol. The low diffusion coefficient value for 1-octanol is in agreement with the RDF data. The diffusion coefficients of the solvents are $4.19 (\pm 0.01) \times 10^{-9} \text{ m}^2/\text{s}$, $2.820 (\pm 0.002) \times 10^{-9} \text{ m}^2/\text{s}$, and $0.12 (\pm 0.01) \times 10^{-9} \text{ m}^2/\text{s}$ for water, methanol, and 1-octanol, respectively. These values are similar to the diffusion coefficient values for pure solvents at 298 K.^{34,48,49} This indicates that Curcumin has no significant effect on the bulk properties of the solvents at infinite dilution conditions.

Simulation of Curcumin in the DME/DMP Mixture in Water. A 50 ns simulation of Curcumin in a box of water with 23 DME and 24 DMP molecules was performed. Figure 7 shows the spatial distribution of DME and DMP molecules throughout the simulation. The distribution indicates preference of DMP toward the hydrophobic part of the Curcumin molecule. DME does not contribute much to the spatial distribution apart from the keto-enol part in the molecule.

During the same simulation, the minimum distance of the center of mass (CoM) of the Curcumin molecule from the CoM of the DME and DMP molecules is shown in Figure 8. As seen in the spatial distribution, the distance distribution also shows that the DMP molecules always tend to stay closer to the Curcumin molecule.

The average number of contacts (N_{cont}) between the Curcumin molecule and the solvent molecules was found to be 2 (± 1) for DME, 3 (± 2) for DMP, and 70 (± 6) for water. As DMP stays closer to Curcumin, the N_{cont} value is significantly higher for DMP than that of DME. Also, the

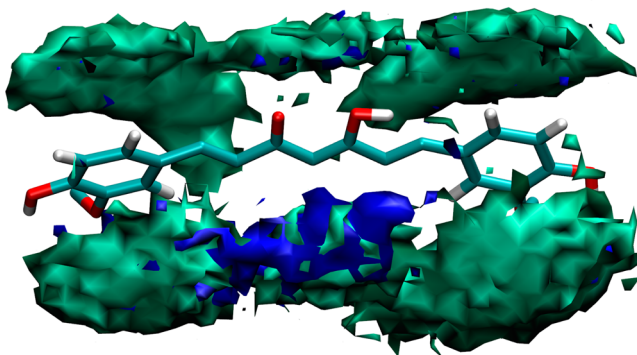


Figure 7. Spatial distribution of DME and DMP molecules around the Curcumin molecule. DME is shown in blue and DMP in green. The density surfaces have an isovalue of 45 for both DME and DMP. For the sake of clarity, water is not shown.

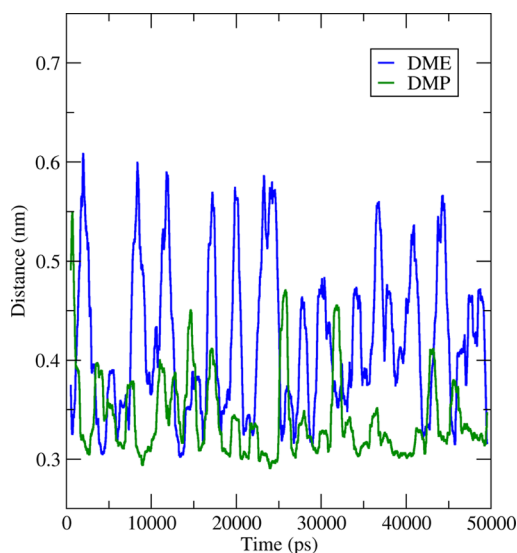


Figure 8. Minimum distance of the DME and DMP molecules from the center of mass of the Curcumin molecule during a 50 ns simulation. A distance cutoff of 0.6 nm was used.

N_{cont} value for Curcumin with water is lower than that of the N_{cont} value in bulk water. This indicates Curcumin's favor toward relatively more hydrophobic molecules when put in a hydrophilic environment. To further support the observation, the RDF for the oxygen atoms of the DME, DMP, and water molecules with respect to the rings of the Curcumin molecule (as shown in Figure 6) was calculated, and it is shown in Figure S4 in the SI. The interactions with the solvents are significantly different at chemically dissimilar parts of the Curcumin molecule. The peak position for the RDF value of DME has the lowest value for the more polar keto-enol ring of the molecule, followed by water and DMP. The trend is quite different for the phenyl rings where the peak position for RDF has the lowest value for DMP, followed by DME and water. The phenyl rings being more hydrophobic than the middle part of the Curcumin molecule favors less hydrophilic DMP molecules than DME or water. The keto-enol part is more polar and favors DME and water over DMP.

The diffusion coefficient value of the Curcumin molecule in the DME/DMP/water mixture was found to be $0.32 (\pm 0.07) \times 10^{-9} \text{ m}^2/\text{s}$, and this value is significantly lower than the values of diffusion coefficients in water and in methanol. This

significant depression in diffusion coefficient value supports the formation of an aggregation with the ether molecules resulting in better solubility and stability in water. Figure 9 shows the trend of diffusion coefficient values of the Curcumin molecule in all the systems simulated.

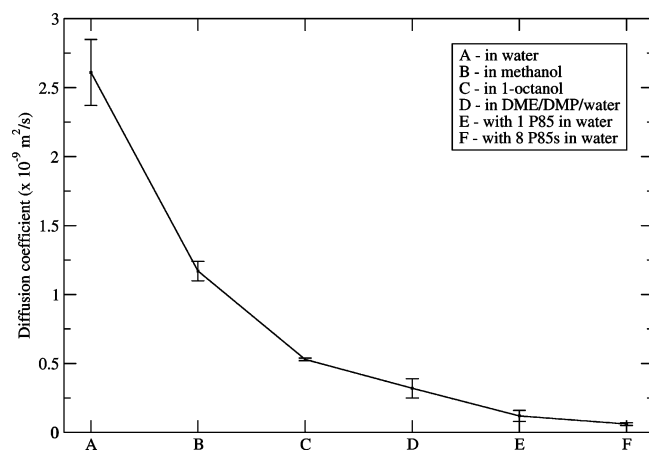


Figure 9. Diffusion coefficient of the Curcumin molecule in different systems simulated. The line is put to help as a visual guide.

Simulation of Curcumin in the Presence of a Single Pluronic P85 Chain

Figure 10 shows the initial and final conformations of Curcumin and one P85 chain from a 50 ns simulation in water. In the initial conformation of the P85 chain, the polymer was taken as a coiled structure. After 50 ns simulation, the PPO part is seen to be still in the coiled conformation close to the Curcumin molecule, whereas the PEO parts stretch in the water. The radius of gyration (R_g) value of the P85 chain was $2.13 \pm 0.40 \text{ nm}$, which is very close to $2.25 \pm 0.04 \text{ nm}$, the R_g value for a single P85 chain in water at 298 K.³⁰ The hydrophobic PPO part of the P85 chain, when put in water, is supposed to form a core, and the hydrophilic PEO parts remain extended in the solvent. In this scenario, we observe a similar behavior. The Curcumin molecule being hydrophobic prefers to stay close to the hydrophobic core of the P85 chain, and as a result, the mobility of the drug molecule is suppressed to a great extent. The diffusion coefficient of the Curcumin molecule was calculated to be $0.12 (\pm 0.04) \times 10^{-9} \text{ m}^2/\text{s}$, which is much less than that of free Curcumin in water (Figure 11).

Figure 11 shows the number of contacts (within 0.6 nm) between the Curcumin molecule with PEO (blue) and PPO

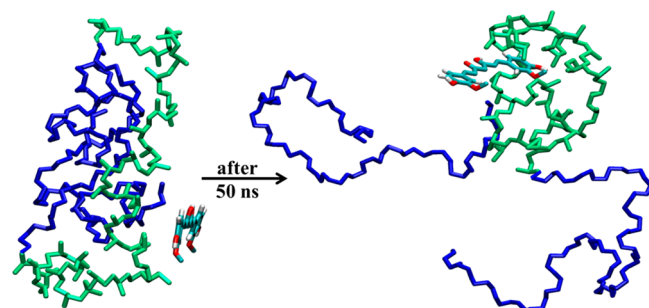


Figure 10. Snapshot of the P85 and the Curcumin molecule at the beginning and at the end of a 50 ns simulation. The PEO part of P85 is shown in blue, and the PPO part is shown in green.

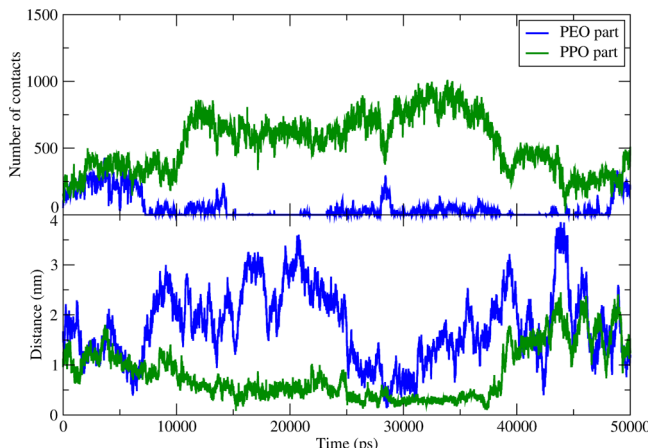


Figure 11. Average number of contacts between the PEO and PPO with the P85 chain is shown in the top. A distance cutoff of 0.6 nm was used. Minimum distance of the PEO part and PPO part of the Pluronic P85 molecule from the center of mass of the Curcumin molecule during a 50 ns simulation is shown in the bottom panel.

(green). The plot shows a significantly higher number of contacts for PPO than that for PEO. In the same figure, the distribution of minimum distance of the PEO and PPO parts of P85 from the center of mass of Curcumin during the simulation of a Curcumin molecule in the presence of one P85 chain in water is shown. Throughout the simulation, the PPO part is seen to be closer to the Curcumin molecule than the PEO parts. This observation goes hand in hand with the findings from the simulation of Curcumin in the presence of DME and DMP. In that case as well, we have observed that the hydrophobic DMP molecules tend to stay close to the Curcumin molecule.

Simulation of Curcumin in the Presence of Multiple Pluronic P85 Chains. Simulation of a single P85 chain with Curcumin shows the potential to form a drug–polymer aggregate. Sahu et al.²⁷ have experimentally studied encapsulation of Curcumin in Pluronic micelles. They have found that in the presence of Curcumin, spherical micelles with sizes in the range of 20–80 nm are formed. Also, fluorescence emission spectra indicated that Curcumin molecules are encapsulated in the hydrophobic core of the micelle and form a stable aggregate. However, no specific information about the composition and formation of the aggregate/micelle is available. To investigate the properties of the aggregation, one Curcumin molecule was simulated in a box of water with eight P85 chains. The initial conformation of the system is shown in Figure S2 in the SI. Figure 12 shows the final conformation of the system. The snapshot shows a hydrophobic core formed with the hydrophobic PPO parts of four P85 chains that wrap the Curcumin molecule, while the hydrophilic PEO parts flank in water. Moreover, it is seen that only four P85 chains take part in formation of an aggregation with the Curcumin molecule. The radius of gyration of the drug–polymer aggregation was found to be 5.0 ± 1.2 nm. As seen for the simulations of Curcumin in the DME/DMP/water mixture and with one P85 chain in water, the hydrophobic interaction between Curcumin and PPO is the main driving force for the formation of the aggregate. The results indicate that the Pluronic P85 can be used as a potential nanocarrier for Curcumin.

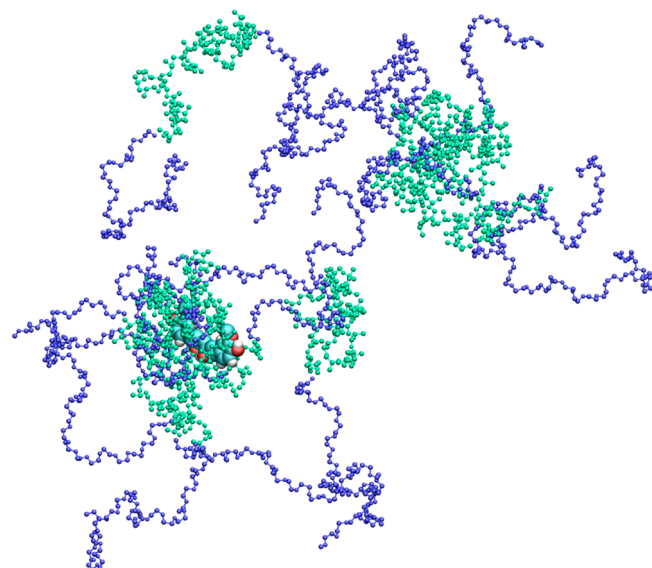


Figure 12. Snapshot of the final conformation of P85 chains around the Curcumin molecule after a 100 ns simulation. The hydrophilic PEO chains are shown in blue, and the hydrophobic PPO chains are shown in green.

Eight P85 chains were also simulated in water in the absence of the Curcumin molecule to check if Curcumin affects the aggregation tendency of the Pluronic chains. Within the same simulation time, aggregation of the polymer chains, monitored as number of contacts along the simulation time, was observed with no major changes in the aggregation tendency (Figure S8 in the SI).

The spatial distribution of PEO and PPO chains around the drug molecule is shown in Figure 13. At the level of the same isovalue, the hydrophobic PPO is seen to form a pocket on one

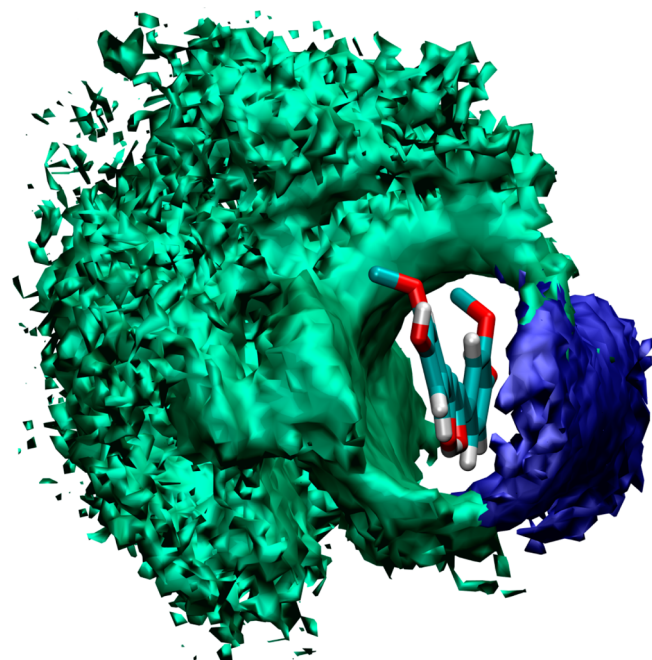


Figure 13. Spatial distribution of PEO and PPO chains around the Curcumin molecule. PEO is shown in blue and PPO in red. The density surfaces have an isovalue of 250 for both PEO and PPO.

side of the Curcumin molecule, and the PEO chains have a relatively smaller contribution toward the spatial distribution. A similar distribution is seen for the spatial distribution of DME and DMP around Curcumin in aqueous solution. The number of hydrogen bonds and the number of pairs within 0.35 nm between water and Curcumin decrease in the presence of P85 chains in comparison to that in bulk water (Figure S5 in the SI). The number of contacts (within 0.6 nm) between water and Curcumin is 2442 in bulk water, but it reduces to 1108 in the presence of P85 chains. These indicate that the stability of the Curcumin molecule in the aggregate is enhanced by reducing its interaction with water in the presence of Pluronic P85.

Also, the diffusion coefficient of the Curcumin molecule in this system is the lowest of all the systems simulated (Figure 9). It has a value of only $0.06 (\pm 0.01) \times 10^{-9} \text{ m}^2/\text{s}$. The aggregation of multiple Pluronic chains around the drug molecule makes mobilization even harder. Strong interaction with the hydrophobic PPO part of the Pluronic P85 and reduced mobility result in slow and sustained release of the drug in physiological conditions. This is particularly advantageous as chemotherapy requires a controlled concentration of drug in blood for a relatively longer period.

CONCLUSIONS

The aim of the present work was the better understanding of the interaction of Curcumin with one of its potential carriers, i.e., PEO–PPO–PEO block copolymers. Molecular dynamics simulations have been used to analyze these interactions at the molecular level. A novel model of Curcumin based on the GROMOS96 force field has been proposed. First, the model was used to study the properties of the molecule in water, methanol, and 1-octanol. Subsequently, DME and DMP in water solution and in the presence of the Pluronic P85 chains was analyzed.

The Curcumin model reproduces in fair agreement the trend of theoretical data of the water/1-octanol partition coefficient. It shows relatively better solvation tendency in methanol than that in 1-octanol and indicates insolubility in water. The trend of free energy of solvation was observed to be $\Delta G_{\text{hyd}} > \Delta G_{\text{oct}} > \Delta G_{\text{met}}$, and it is consistent with the existing knowledge of the chemical nature of Curcumin.

In the presence of DME and DMP molecules, the more hydrophobic DMP molecules preferentially coat the Curcumin. The same behavior was observed in the presence of single and multiple P85 chains in water. In the case of P85, the hydrophobic PPO chains wrap around the Curcumin molecule leaving the PEO parts exposed and thus resulting in better solvation and stability of the drug molecule in water. This also affects the mobility of the drug molecule by decreasing its diffusion coefficient. The formation of drug–polymer aggregation is observed within 100 ns of simulation. This observed condensing nuclei could be the first step to form the larger micelle observed in the experimental study reported in the literature.

ASSOCIATED CONTENT

Supporting Information

Details of the optimized structure of Curcumin, force field parameters, starting conformations for simulations, dH/dl curves, and RDF plots. This material is available free of charge via the Internet at <http://pubs.acs.org>.

AUTHOR INFORMATION

Corresponding Author

*Fax: +49 421 200-3249. Tel.: +49 421 200-3144. E-mail: d.roccatano@jacobs-university.de.

Notes

The authors declare no competing financial interest.

ACKNOWLEDGMENTS

This project is funded by the Deutsche Forschungsgemeinschaft (DFG) for the project “The study of detailed mechanism of polymers/biological membrane interactions using computer simulation” (RO 3571/3-1). The computational resources of the Computer Laboratories for Animation, Modeling and Visualization (CLAMV) at Jacobs University Bremen were used for the study.

REFERENCES

- (1) Turmeric and Curcumin. In *WHO Food Additives Series 6*; World Health Organization: Geneva, 1975.
- (2) Govindarajan, V. S.; Stahl, W. H. Turmeric - Chemistry, Technology, and Quality. *C.R.C. Crit. Rev. Food Sci. Nutr.* **1980**, *12*, 199–301.
- (3) Padma, T. V. Ayurveda. *Nature* **2005**, *436*, 486–486.
- (4) Shishodia, S.; Sethi, G.; Aggarwal, B. B. Curcumin: Getting Back to the Roots. *Ann. N.Y. Acad. Sci.* **2005**, *1056*, 206–217.
- (5) Notarbartolo, M.; Poma, P.; Perri, D.; Dusonchet, L.; Cervello, M.; D'Alessandro, N. Antitumor Effects of Curcumin, Alone or in Combination with Cisplatin or Doxorubicin, on Human Hepatic Cancer Cells. Analysis of their Possible Relationship to Changes in NF- κ B Activation Levels and in IAP Gene Expression. *Cancer Lett.* **2005**, *224*, 53–65.
- (6) Kuo, M. L.; Huang, T. S.; Lin, J. K. Curcumin, an Antioxidant and Anti Tumor Promoter, Induces Apoptosis in Human Leukemia Cells. *Biochim. Biophys. Acta* **1996**, *1317*, 95–100.
- (7) Sharma, R. A.; Gescher, A. J.; Steward, W. P. Curcumin: The Story So Far. *Eur. J. Cancer* **2005**, *41*, 1955–1968.
- (8) Aggarwal, B. B.; Kumar, A.; Bharti, A. C. Anticancer Potential of Curcumin: Preclinical and Clinical Studies. *Anticancer Res.* **2003**, *23*, 363–398.
- (9) Kunnumakkara, A. B.; Guha, S.; Krishnan, S.; Diagaradjane, P.; Gelovani, J.; Aggarwal, B. B. Curcumin Potentiates Antitumor Activity of Gemcitabine in an Orthotopic Model of Pancreatic Cancer through Suppression of Proliferation, Angiogenesis, and Inhibition of Nuclear Factor- κ B-Regulated Gene Products. *Cancer Res.* **2007**, *67*, 3853–3861.
- (10) Singh, S.; Aggarwal, B. B. Activation of Transcription Factor NF-B Is Suppressed by Curcumin (Diferuloylmethane). *J. Biol. Chem.* **1995**, *270*, 24995–25000.
- (11) Bharti, A. C.; Aggarwal, B. B. Nuclear Factor- κ B and Cancer: Its Role in Prevention and Therapy. *Biochem. Pharmacol.* **2002**, *64*, 883–888.
- (12) Ringman, J. M.; Frautschy, S. A.; Cole, G. M.; Masterman, D. L.; Cummings, J. L. A Potential Role of the Curry Spice Curcumin in Alzheimer's Disease. *Curr. Alzheimer Res.* **2005**, *2*, 131–136.
- (13) Cole, G. M.; Morihara, T.; Lim, G. P.; Yang, F.; Begum, A.; Frautschy, S. A. NSAID and Antioxidant Prevention of Alzheimer's Disease: Lessons from In Vitro and Animal Models. *Ann. N.Y. Acad. Sci.* **2004**, *1035*, 68–84.
- (14) Zhao, L. N.; Chiu, S.-W.; Benoit, J.; Chew, L. Y.; Mu, Y. The Effect of Curcumin on the Stability of $\text{A}\beta$ Dimers. *J. Phys. Chem. B* **2012**, *116*, 7428–7435.
- (15) Tønnesen, H. H.; Másson, M.; Loftsson, T. Studies of Curcumin and Curcuminoids. XXVII. Cyclodextrin Complexation: Solubility, Chemical and Photochemical Stability. *Int. J. Pharm.* **2002**, *244*, 127–135.
- (16) Tønnesen, H. H.; Karlsen, J. Studies on Curcumin and Curcuminoids. *Z. Lebensm. Forsch. A* **1985**, *180*, 402–404.

- (17) Shoba, G.; Joy, D.; Joseph, T.; Majeed, M.; Rajendran, R.; Srinivas, P. S. S. R. Influence of Piperine on the Pharmacokinetics of Curcumin in Animals and Human Volunteers. *Planta Med.* **1998**, *64*, 353–356.
- (18) Ireson, C.; Orr, S.; Jones, D. J. L.; Verschoyle, R.; Lim, C.-K.; Luo, J.-L.; Howells, L.; Plummer, S.; Jukes, R.; Williams, M.; Steward, W. P.; Gescher, A. Characterization of Metabolites of the Chemopreventive Agent Curcumin in Human and Rat Hepatocytes and in the Rat in Vivo, and Evaluation of Their Ability to Inhibit Phorbol Ester-induced Prostaglandin E2 Production. *Cancer Res.* **2001**, *61*, 1058–1064.
- (19) Kabanov, A. V.; Batrakova, E. V.; Alakhov, V. Y. Pluronic® Block Copolymers as Novel Polymer Therapeutics for Drug and Gene Delivery. *J. Controlled Release* **2002**, *82*, 189–212.
- (20) Schmolka, I. R. Polymers for Controlled Drug Delivery. In *Polymers for Controlled Drug Delivery*; Tarcha, P. J., Ed.; CRC Press: Boston, 1991.
- (21) Oh, K. T.; Bronich, T. K.; Kabanov, A. V. Micellar Formulations for Drug Delivery Based on Mixtures of Hydrophobic and Hydrophilic Pluronic® Block Copolymers. *J. Controlled Release* **2004**, *94*, 411–422.
- (22) Ma, Z.; Haddadi, A.; Molavi, O.; Lavasanifar, A.; Lai, R.; Samuel, J. Micelles of Poly(ethylene oxide)-b-poly(ϵ -caprolactone) as Vehicles for the Solubilization, Stabilization, and Controlled Delivery of Curcumin. *J. Biomed. Mater. Res., Part A* **2008**, *86A*, 300–310.
- (23) Sahu, A.; Bora, U.; Kasoju, N.; Goswami, P. Synthesis of Novel Biodegradable and Self-Assembling Methoxy Poly(ethylene glycol)-palmitate Nanocarrier for Curcumin Delivery to Cancer Cells. *Acta Biomater.* **2008**, *4*, 1752–1761.
- (24) Vakil, R.; Kwon, G. S. Poly(ethylene glycol)-b-poly(epsilon-caprolactone) and PEG-Phospholipid Form Stable Mixed Micelles in Aqueous Media. *Langmuir* **2006**, *22*, 9723–9729.
- (25) Zahr, A. S.; de Villiers, M.; Pishko, M. V. Encapsulation of Drug Nanoparticles in Self-Assembled Macromolecular Nanoshells. *Langmuir* **2005**, *21*, 403–410.
- (26) Das, R. K.; Kasoju, N.; Bora, U. Encapsulation of Curcumin in Alginate-Chitosan-Pluronic Composite Nanoparticles for Delivery to Cancer Cells. *Nanomed. Nanotechnol.* **2009**, *6*, 153–160.
- (27) Sahu, A.; Kasoju, N.; Goswami, P.; Bora, U. Encapsulation of Curcumin in Pluronic Block Copolymer Micelles for Drug Delivery Applications. *J. Biomater. Appl.* **2011**, *25*, 619–639.
- (28) Melik-Nubarov, N. S.; Pomaz, O. O.; Dorodnych, T. Y.; Badun, G. A.; Ksenofontov, A. L.; Schemchukova, O. B.; Arzhakov, S. A. Interaction of Tumor and Normal Blood Cells with Ethylene Oxide and Propylene Oxide Block Copolymers. *FEBS Lett.* **1999**, *446*, 194–198.
- (29) Batrakova, E. V.; Dorodnych, T. Y.; Klinskii, E. Y.; Kliushnenkova, E. N.; Shemchukova, O. B.; Goncharova, O. N.; Arjakov, S. A.; Alakhov, V. Y.; Kabanov, A. V. Anthracycline Antibiotics Non-Covalently Incorporated into the Block Copolymer Micelles: In Vivo Evaluation of Anticancer Activity. *Br. J. Can.* **1996**, *74*, 1545–1552.
- (30) Hezaveh, S.; Samanta, S.; Milano, G.; Roccatano, D. Molecular Dynamics Simulation Study of Solvent Effects on Conformation and Dynamics of Polyethylene Oxide and Polypropylene Oxide Chains in Water and in Common Organic Solvents. *J. Chem. Phys.* **2012**, *136*, 124901–124912.
- (31) Khopde, S. M.; Indira Priyadarsini, K.; Palit, D. K.; Mukherjee, T. Effect of Solvent on the Excited-State Photophysical Properties of Curcumin. *Photochem. Photobiol.* **2000**, *72*, 625–631.
- (32) Breneman, C. M.; Wiberg, K. B. Determining Atom-Centered Monopoles from Molecular Electrostatic Potentials. The Need for High Sampling Density in Formamide Conformational Analysis. *J. Comput. Chem.* **1990**, *11*, 361–373.
- (33) Samanta, S.; Hezaveh, S.; Milano, G.; Roccatano, D. Diffusion of 1,2-Dimethoxyethane and 1,2-Dimethoxypropane through Phosphatidylcholine Bilayers: A Molecular Dynamics Study. *J. Phys. Chem. B* **2012**, *116*, 5141–5151.
- (34) Hezaveh, S.; Samanta, S.; Milano, G.; Roccatano, D. Structure and Dynamics of 1,2-Dimethoxyethane and 1,2-Dimethoxypropane in Aqueous and Non-Aqueous Solutions: A Molecular Dynamics Study. *J. Chem. Phys.* **2011**, *135*, 164501–164511.
- (35) Berendsen, H. J. C.; Postma, J. P. M.; van Gunsteren, W. F.; Hermans, J. In *Intermolecular Forces*; Pullman, B., Ed.; Reidel: Dordrecht, 1981; p 331.
- (36) Jorgensen, W. L.; Maxwell, D. S.; TiradoRives, J. Development and Testing of the OPLS All-Atom Force Field on Conformational Energetics and Properties of Organic Liquids. *J. Am. Chem. Soc.* **1996**, *118*, 11225–11236.
- (37) Garrido, N. M.; Queimada, A. J.; Jorge, M.; Macedo, E. A.; Economou, I. G. 1-Octanol/Water Partition Coefficients of n-Alkanes from Molecular Simulations of Absolute Solvation Free Energies. *J. Chem. Theory Comput.* **2009**, *5*, 2436–2446.
- (38) Frisch, M. J.; Trucks, G. W.; Schlegel, H. B.; Scuseria, G. E.; Robb, M. A.; Cheeseman, J. R.; Montgomery, J. A.; Vreven, T.; Kudin, K. N.; Burant, J. C.; et al. *Gaussian 03*, Revision C.02; Gaussian, Inc.: Wallingford, CT, 2003.
- (39) Hess, B.; Kutzner, C.; van der Spoel, D.; Lindahl, E. GROMACS 4: Algorithms for Highly Efficient, Load-Balanced, and Scalable Molecular Simulation. *J. Chem. Theory Comput.* **2008**, *4*, 435–447.
- (40) Humphrey, W.; Dalke, A.; Schulter, K. VMD: Visual Molecular Dynamics. *J. Mol. Graphics* **1996**, *14*, 33–38.
- (41) Bussi, G.; Donadio, D.; Parrinello, M. Canonical Sampling through Velocity Rescaling. *J. Chem. Phys.* **2007**, *126*, 14101–14107.
- (42) Berendsen, H. J. C.; Postma, J. P. M.; Vangunsteren, W. F.; Dinola, A.; Haak, J. R. Molecular-Dynamics with Coupling to an External Bath. *J. Chem. Phys.* **1984**, *81*, 3684–3690.
- (43) Hess, B.; Bekker, H.; Berendsen, H. J. C.; Fraaije, J. G. E. M. LINCS: A Linear Constraint Solver for Molecular Simulations. *J. Comput. Chem.* **1997**, *18*, 1463–1472.
- (44) Darden, T.; York, D.; Pedersen, L. Particle Mesh Ewald - an N.Log(N) Method for Ewald Sums in Large Systems. *J. Chem. Phys.* **1993**, *98*, 10089–10092.
- (45) Kirkwood, J. Statistical Mechanics of Fluid Mixtures. *J. Chem. Phys.* **1935**, *3*, 300–313.
- (46) ACD/Labs *Advanced Chemistry Development Software*, V11.02; Advanced Chemistry Development, Inc.: Toronto, On, Canada, 1994–2012.
- (47) Fujisawa, S.; Ishihara, M.; Murakami, Y.; Atsumi, T.; Kadoma, Y.; Yokoe, I. Predicting the Biological Activities of 2-Methoxyphenol Antioxidants: Effects of Dimers. *In Vivo* **2007**, *21*, 181–188.
- (48) Mark, P.; Nilsson, L. Structure and Dynamics of the TIP3P, SPC, and SPC/E Water Models at 298 K. *J. Phys. Chem. A* **2001**, *105*, 9954–9960.
- (49) Marcus, Y. *The Properties of Solvents*; Wiley: Chichester; New York, 1998; p 239.